# Ion-specific thermodynamics of multicomponent electrolytes: A hybrid HNC/MD approach

**ARTICLE** *in* THE JOURNAL OF CHEMICAL PHYSICS · OCTOBER 2009

Impact Factor: 2.95 · DOI: 10.1063/1.3248218 · Source: PubMed

# Ion-specific thermodynamics of multicomponent electrolytes: a hybrid HNC/MD approach

Luboš Vrbka* and Werner Kunz

*Institut für Physikalische und Theoretische Chemie*

*Universität Regensburg*

*93040 Regensburg, Germany*

Mikael Lund†

*Department of Theoretical Chemistry*

*Lund University*

*p.o. Box 124*

*SE-22100 Lund, Sweden*

Immanuel Kalcher, Joachim Dzubiella, and Roland R. Netz‡

*Physik Department (T37)*

*Technische Universität München*

*85748 Garching, Germany*

(Dated: September 1, 2009, revised manuscript)

# Abstract

Using effective infinite dilution ion-ion interaction potentials derived from explicit-water molecular dynamics (MD) computer simulations in the hypernetted-chain (HNC) integral equation theory we calculate the liquid structure and thermodynamic properties, namely the activity and osmotic coeffcients of various multicomponent aqueous electrolyte mixtures. The electrolyte structure expressed by the ion-ion radial distribution functions is for most ions in excellent agreement with MD and implicit solvent Monte-Carlo (MC) simulation results. Calculated thermodynamic properties are also represented consistently among these three methods. Our versatile HNC/MD hybrid method allows for a quick prediction of the thermodynamics of multicomponent electrolyte solutions for a wide range of concentrations and an efficient assessment of the validity of the employed MD force-fields with possible implications in the development of thermodynamically consistent parameter sets.



Keywords: molecular dynamics, integral equation theory, hypernetted-chain approximation, potential of mean force, osmotic coefficient

## INTRODUCTION

Ions play an indispensable role in many natural, biological, and technological processes. It is, therefore, not surprising that the evaluation and description of properties of electrolyte solutions has gathered a lot of interest since more than 100 years. Nevertheless, despite the tremendous effort, our understanding of this topic is still far from being complete.

As an important foundation, the Debye-Hückel (DH) theory of electrolytes [1] provided a basic description of very dilute solutions. Its importance lies in the fact that the more complex methods reduce to the DH description in the limit of infinite dilution. For practical purposes, a plethora of more advanced approaches has been derived. First improvements came from the extension of the DH law with additional terms, broadening the concentration range where this method is valid. Pitzer presented a frequently used extension of this theory using semiempirical equations [2].

Another approach, the so-called Mean Spherical Approximation (MSA), combining Coulombic interactions and hard sphere potentials (whereas limiting DH describes ions as point charges), still belongs among the most popular primitive models, in which the solvent is treated as a continuum [3–7]. A more refined continuum model, based on the hypernetted chain equation (HNC) was proposed by Friedman and coworkers [8]. Patey *et al.* used the machinery of integral equations for a very sophisticated description of electrolyte solutions [9, 10]. More recent attempts combine physics-based models with the engineers' needs of practicable fitting equations [6, 11–13].

The inherent problem of these methods is the requirement of usage of fitting parameters in order to provide results both qualitatively and quantitatively consistent with experimental findings. These adjustable parameters often cannot be associated with any physical measurable quantity. Therefore, transfer of such parameters between different systems is usually not possible.

Molecular dynamics (MD) and Monte Carlo (MC) simulation methods, which can work at various levels of detail (full atomic treatment or coarse-grained approaches) belong to the alternatives. Their main disadvantage lies in the large computing time costs and inability to study systems at very low concentrations, particularly for simulations involving explicitly resolved solvent molecules. This also means that the evaluation of thermodynamic properties or the testing/optimization of the underlying interaction parameter set (the so-called

'force-field') in the simulation is complicated and rather time consuming. Typically a long simulation is needed for every salt concentration of interest. Several succesful attempts are, however, known from the literature [14–19].

We propose here another approach towards the theoretical prediction of thermodynamic properties. A single explicit solvent MD simulation at low but finite concentration is performed for the given salt using a reliable or to-be-tested force field and the solvent-averaged potential of mean force (PMF) at *infinite dilution* of the ions is extracted using the procedure described in the methodological section. This PMF is then used as an effective pair potential in the solvent-averaged integral equation approach (the HNC approximation in our case), which is extremely time efficient and allows for easy evaluation of thermodynamic properties for a wide range of concentrations. For the purpose of validation of the integral equation method, we also perform a primitive-model (implicit solvent) MC calculation employing the same effective pair potential in the same concentration range. As MC is inherently exact at the primitive level, HNC can be tested for providing reliable data.

We are aware of some similar approaches reported in the literature. In all cases, the usage of the combination of a simulation method and HNC integral equation lead to very plausible results. Kunz *et al.* fitted solvent-averaged ion pair potentials for the description of tetrapentylammonium ions in acetonitrile, which were used in Brownian Dynamics in order to estimate the diffusion coefficients. The HNC was used in the fitting process in order to keep the pair potential consistent with thermodynamics and scattering data [20]. In their recent work, Krienke *et al.* used the explicit solvent MD simulations for obtaining the distribution functions for tetraalkylammonium halide salts in water [21]. These functions were then converted (fitted) to the solvent-averaged pair potentials using Coulombic, hard sphere, and square well interactions.

The present study, on the other hand, does not involve any fitting. The infinite dilution PMFs of the respective ions originating from explicit solvent MD simulation are used directly in the implicit solvent HNC calculations at a wide range of concentrations (0-2 mol/l). The structural (pair correlation functions) as well as the thermodynamic (osmotic and activity coefficients) properties are described consistently between MD and HNC. Further comparison with the results of implicit solvent MC calculations using the same effective potentials shows that HNC and MC provide essentially the same answers in the concentration range used for this work.

This outcome is in agreement with the work of Lyubartsev and Marčelja [22], who attempted to extract the effective ion-ion interaction potentials from the full molecular molecular dynamics simulations. Two different approaches used for this purpose – inverse Monte Carlo calculation and (effective) HNC approximation – showed excellent agreement, supporting the suitability of the combination of HNC with effective pair potentials for the description of aqueous ionic solutions.

## METHODOLOGY

For the purpose of this work, we developed pyOZ – a versatile numerical solver of the Ornstein-Zernike equation in the Python programming language, using the open-source numerical library SciPy [23]. The program can be downloaded and all features are documented on the project homepage [24].

### HNC integral equation theory

We perform our calculations at the McMillan-Mayer (MM) level [25], taking the solvent into account in an averaged way by means of a concentration-dependent dielectric constant $\epsilon(c)$ (solvent-averaged primitive model). The well-established hypernetted chain (HNC) approximation (closure) relates the pair correlation function $g_{ij}(r)$ between two particles $i$, $j$ to the pair potential $U_{ij}(r)$ by [26]

$$g_{ij}(r) = \exp\left(-\beta U_{ij}(r) + \gamma_{ij}(r)\right), \tag{1}$$

where $\beta = 1/kT$ is the inverse thermal energy, $\gamma_{ij} = h_{ij}(r) - c_{ij}(r)$ is the indirect correlation function, and the total correlation function $h_{ij}(r)$ is defined as $h_{ij}(r) = g_{ij}(r) - 1$. Rearrangement of Eq. 1 leads to the HNC closure in the form involving the direct correlation function $c_{ij}(r)$:

$$c_{ij}(r) = \exp\left(-\beta U_{ij}(r) + \gamma_{ij}(r)\right) - \gamma_{ij}(r) - 1. \tag{2}$$

From now on, the dependence on the separation will be implicitly assumed in order to simplify the equations, so that the argument will be dropped in the following.

The Ornstein-Zernike (OZ) equation [27] for a $N$-component mixtufure with particle

number densities $\rho_n$ reads

$$h_{ij} = c_{ij} + \sum_n^N \rho_n \int c_{in} h_{nj} d\vec{r}_n \tag{3}$$

involving the convolution integral of direct and total correlation functions. A straightforward approach to the solution of this equation involves the Fourier transformation (FT, denoted by the hat sign; recall that the FT of a convolution is a simple product of FTs of individual functions). The FT is normalized to the particle densities in order to have dimensionless correlation functions in the Fourier space. The forward transformation then involves multiplication with density prefactors (*e.g.*, $\hat{H}_{ij} = \sqrt{\rho_i \rho_j}\hat{h}_{ij}$), the inverse transformation involves division by the same factors.

Fourier space expressions for $h_{ij}$ and $\gamma_{ij}$ in matrix notation then read

$$\hat{\mathbb{H}} = \hat{\mathbb{C}} + \hat{\mathbb{C}} \cdot \hat{\mathbb{H}} \tag{4}$$

$$\hat{\Gamma} = \hat{\mathbb{H}} - \hat{\mathbb{C}} = \left(\hat{\mathbb{E}} - \hat{\mathbb{C}}\right)^{-1} \hat{\mathbb{C}} - \hat{\mathbb{C}}, \tag{5}$$

with $\hat{\Gamma}$ being the vector of indirect correlation functions in the Fourier space and $\mathbb{E}$ being the identity matrix.

The solution procedure is iterative. At the beginning, it involves choosing some initial value $\gamma^{\text{in}}$ for the functions $\gamma_{ij}$ (zero or $\gamma_{ij}$ from a previous calculation is often used as a starting point). Using Eq. 2, the direct correlation functions in the real space are calculated using the HNC closure and then Fourier-transformed, the matrix problem (Eq. 5) is solved and the resulting functions $\hat{\Gamma}_{ij}$ are transformed back. If the calculation has not converged, the result ($\gamma^{\text{out}}$) is mixed with the input ($\gamma^{\text{in}}$) and used in the next iteration. We are using the root mean square of the differences between $\gamma^{\text{in}}$ and $\gamma^{\text{out}}$ normalized to the number of components and discretization points as a convergence criterion.

This straightforward procedure is slightly complicated by the fact that we work with long-ranged potentials (Coulombic interaction between the ions), whose FTs are divergent and pose, therefore, a problem to the numerical FT routines. We apply here the procedure of Ng [28], who suggested transforming the long-ranged functions $U_{ij}$, $C_{ij}$ and $\Gamma_{ij}$ to short ranged functions using a suitable well-behaved reference function $U^{\text{c}}_{ij}$ as follows

$$U^{\text{Ng}}_{ij} = U_{ij} - U^{\text{c}}_{ij} \tag{6}$$

$$c^{\text{Ng}}_{ij} = c_{ij} + U^{\text{c}}_{ij} \tag{7}$$

$$\gamma^{\text{Ng}}_{ij} = \gamma_{ij} - U^{\text{c}}_{ij} = h_{ij} - c^{\text{Ng}}_{ij}. \tag{8}$$

Sought is a reference function that is capable of counteracting the long range tail of our pair potential. For potentials in the form $U = A/r$, one of the possibilities is

$$U_{ij}^{\mathrm{c}}(r) = (A_{ij}/r)\ \mathrm{erf}(\alpha r), \tag{9}$$

whose analytical FT reads ($k$ is the wave vector)

$$\hat{U}_{ij}^{\mathrm{c}}(k) = \frac{A}{k^2} 4\pi \exp\left(-\frac{k^2}{4\alpha^2}\right), \tag{10}$$

with $\alpha$ being an adjustable parameter. The iteration procedure has to be modified so that the reference function is added to the calculated $c_{ij}$, the resulting short-range function is Fourier-transformed and then the FT of the reference function (Eq. 10) is subtracted from the result. The matrix problem (Eq. 5) is then solved and new short-ranged $\hat{\gamma}_{ij}^{\mathrm{Ng}}$ is calculated using Eq. 8. After transformation to the real space and reconstruction of the long-ranged $\gamma_{ij}$, the algorithm returns to the beginning of the iterative cycle.

**Osmotic coefficients**

The osmotic coefficient $\Phi$ of a salt is a measure for the activity of water $a_w$ in a solution and can be calculated from

$$\Phi = -\frac{n_w}{\nu n_s} \ln a_w, \tag{11}$$

where $n_s$ and $n_w$ are molar amounts of salt and water, respectively, and $\nu$ is number of components originating from dissolution of the solute in water (*e.g.*, 2 for NaCl). The equivalent statistical thermodynamical expression [29] not taking the many-body effects due to water into account, which can be derived from the virial equation of state (the *virial route*) reads

$$\Phi = \frac{\Pi}{\rho k T} = 1 - \frac{\beta}{6} \sum_{i,j} \rho_i \rho_j \int_0^\infty r \frac{\partial U_{ij}}{\partial r} g_{ij}(r) 4\pi r^2 dr, \tag{12}$$

where $\Pi$ is the electrolyte osmotic pressure. The total pair potential $U_{ij}$, i.e., the interaction between particles $i$ and $j$ at infinite dilution of both can be written as a sum of contributions of its constituent interaction types (*e.g.*, Coulomb, Lennard-Jones, dispersion, ...),

$$U_{ij} = \sum_n U_{ij}^{(n)}, \tag{13}$$

leading to

$$\Phi = 1 + \sum_n \frac{2\pi}{3\rho} \sum_{i,j} \rho_i \rho_j \int_0^\infty \frac{\partial(-\beta U_{ij}^{(n)})}{\partial r} g_{ij} r^3 dr = 1 + \sum_n \phi^{(n)}, \tag{14}$$

defining the contribution $\phi^{(n)}$ of a given potential $U_{ij}^{(n)}$ to the total osmotic coefficient $\Phi$. The most problematic part of this expression is the derivative of the pair interaction $U_{ij}^{(n)}$. Particularly for non-analytic potentials, which must be evaluated numerically, it is better to use the following procedure to obtain more stable solutions.

We write the pair correlation function in the HNC approximation as a product of factors $g_{ij}^{(n)}$, corresponding to the pair correlation function of individual constituents of the total potential.

$$g_{ij} = \mathrm{e}^{\gamma_{ij} + \sum_n -\beta U_{ij}^{(n)}} = \mathrm{e}^{\gamma_{ij}} \prod_n \mathrm{e}^{-\beta U_{ij}^{(n)}} = \mathrm{e}^{\gamma_{ij}} \prod_n g_{ij}^{(n)} \tag{15}$$

Thus, we are separating the contributions of the pair potential (direct interaction) and of the indirect correlation function $\gamma$. Using the properties of the derivative of the functions $g_{ij}^{(n)}$, which is (for nonanalytic potentials) much more numerically stable than the derivative of $U_{ij}^{(n)}$, it then follows that

$$\phi^n = \frac{2\pi}{3\rho} \sum_{i,j} \rho_i \rho_j \int_0^\infty \frac{\partial g_{ij}^{(n)}}{\partial r} \mathrm{e}^{\gamma_{ij}} \left( \prod_{m \neq n} g_{ij}^{(m)} \right) r^3 dr. \tag{16}$$

Whether the expression involving the derivative of the pair potential (Eq. 14) or the derivative of the pair correlation function (Eq. 16) is used depends on the character of the potential. The latter is generally used for non-analytic potentials. On the other hand, using the former expression with potentials with analytical derivatives leads often to simplifications of the resulting formulae.

An alternative approach to the osmotic coefficients utilizes the so-called *compressibility route*. As was discussed in more detail by Kalcher and Dzubiella [19], the osmotic coefficient $\Phi$ (Eq. 12) can be obtained by an integration of the compressibility $\chi_T$ via

$$\chi_T = \left( \rho \frac{\partial \Pi}{\partial \rho} \right)^{-1}. \tag{17}$$

The statistical mechanical expression for the excess isothermal compressibility $\chi_T^{\mathrm{ex}}$ is then [30]

$$(\chi_T^{\mathrm{ex}})^{-1} = \frac{\chi_T^\circ}{\chi_T} = 1 - \sum_i \sum_j \frac{\rho_i \rho_j}{\rho} \int_0^\infty c_{ij}^s 4\pi r^2 dr, \tag{18}$$

with $\rho = \sum_n \rho_n$ being the total particle number density, sums going over all components of the system, $\chi_T^\circ = \beta/\rho$ being the compressibility of the ideal gas, and $c_{ij}^s$ being the short-ranged direct correlation function:

$$c_{ij}^s = c_{ij} + \beta U_{ij}^{\mathrm{coul}} \tag{19}$$

The long ranged part of $c_{ij}$ is given by $-\beta U_{ij}^{\mathrm{coul}}$ [26]. It is sufficient to take only the short-ranged part of the direct correlation function into account in the integration, since the long-ranged contributions vanish due to electroneutrality.

The compressibility equation (Eq. 18) is a multicomponent generalization to the expression involving the Kirkwood-Buff integrals (valid for binary solution of a symmetric electrolyte) given in [19]. Evaluation of the osmotic coefficient using this route then involves a series of calculations at different salt concentrations ($c = \rho/2$ in case of a symmetric binary electrolyte), calculating the corresponding compressibilities, integrating the $\chi_T$ vs. $\rho$ curve and finally obtaining $\Phi$.

**Activity coefficients**

Evaluating the activity coefficient of a given species within the framework of the OZ-equation is generally a complex task [31]. It turns out, however, that in the HNC approximation, the excess chemical potential $\mu_i^{\mathrm{ex}}$ of the component $i$ in the solution can be calculated from a simple expression [30, 32]

$$\beta\mu_i^{\mathrm{ex}} = \sum_j \rho_j \int_0^\infty \left( \frac{h_{ij}\gamma_{ij}}{2} - c_{ij}^s \right) 4\pi r^2 dr, \tag{20}$$

with the sum going over all components of the mixture. The short-ranged direct correlation function $c_{ij}^s$ is defined by Eq. 19. The activity coefficient of the respective component $\gamma_i$ is then

$$\gamma_i = \exp(\beta\mu_i^{\mathrm{ex}}). \tag{21}$$

For binary mixtures, the calculated values for cation $\gamma_+$ and anion $\gamma_-$ are then used for obtaining the ionic mean activity coefficient $\gamma_\pm$ from

$$\gamma_\pm = \sqrt{\gamma_+\gamma_-}. \tag{22}$$

Commonly, the reference state for measured activity coefficients is at infinite dilution ($c = 0$). That is, the excess chemical potential is the free energy change of transferring

a species from infinite dilution to a solution with a finite solute concentration. A salt dependent dielectric constant $\epsilon_r(c)$, used in our study and discussed in more detail in the section devoted to ion-ion pair potentials, implies a Born contribution to the excess chemical potential,

$$\beta\mu_{i,sol}^{\mathrm{ex}} = \frac{l_B z_i^2}{2a_i}\left(\frac{1}{\epsilon_r(c)} - \frac{1}{\epsilon_r(0)}\right) \tag{23}$$

where $a_i$ is the radius of species $i$ and $l_B = \beta e^2/4\pi\epsilon_0$ is the Bjerrum length in vacuum.

For a 1:1 salt, $MX$, the solvation contribution to the mean activity coefficient then becomes

$$\gamma_{\pm,sol} = \exp\left(\frac{\beta\mu_{M,sol}^{\mathrm{ex}} + \beta\mu_{X,sol}^{\mathrm{ex}}}{2}\right) \tag{24}$$

which must be multiplied with the two-particle contribution (Eq. 22) in order to obtain the total mean activity coefficient. If $\epsilon_r(c) < \epsilon_r(0)$ the solvation term of course contributes with a positive free energy ($\gamma_{\pm,sol} > 1$).

As will be shown later, the selection of the radius $a_i$ can have a rather profound effect on the resulting activity coefficient.

In our study, we used two different sets of radii, summarized in Table I – effective radii of the solvated ions (position of the first peak in the respective ion-water oxygen $g(r)$ from explicit solvent MD simulations [19]) and radii of ions including the first solvation shell (position of the second peak in the same $g(r)$).

**Conversion of thermodynamic quantities**

Let us now discuss the comparability of experimental values and the results of the calculations. Experiments (but also molecular simulations employing explicit solvent) treat the system at the so-called Lewis-Randall (LR) level. At the McMillan-Mayer (solvent averaged) level of theory, the thermodynamic functions are calculated at the constant chemical potential of the solvent. As a consequence, LR and MM correspond to different ensembles - the pressure is given by the pressure of the solution (LR) and by the pressure of the pure solvent in equilibrium with the solution (MM), respectively. It is, therefore, necessary to perform conversions in order to be able to compare the results. The resulting expressions

for osmotic and mean activity coefficients [33] are

$$\Phi^{\mathrm{MM}} = \Phi^{\mathrm{LR}}(1+mM_s)\frac{\rho_0}{\rho} = \Phi^{\mathrm{LR}}\frac{m\rho_0}{c} \tag{25}$$

$$\gamma_{\pm}^{\mathrm{MM}} = \gamma_{\pm}^{\mathrm{LR}}(1+mM_s)\frac{\rho_0}{\rho} = \gamma_{\pm}^{\mathrm{LR}}\frac{m\rho_0}{c}, \tag{26}$$

with $m$ and $c$ being molality and molarity of the solution, $M_s$ the molar mass of the solute, $\rho_0$ and $\rho$ densities of the pure solvent and the solution, respectively.

There exist rigorous equations for the purpose of these conversions derived by Friedman [34]. They require knowledge of the compressibility of the solution (which is known only for a few salts). Simonin [35] provided approximate expressions using the partial molal volume of the solution (obtained from the density) and neglecting the compressibility. It was shown, however, that the approach demonstrated by Eqns. 25 and 26 provides sufficiently exact results for 1:1 and 2:1 salts up to the concentrations of 2 M [36, 37].

In this study, the osmotic and mean activity coefficients calculated using the primitive model are converted by means of Eqns. 25 and 26 to the LR level for the purpose of comparison with the experimental and explicit solvent MD data.

**Ion-ion pair potentials and many-body effects**

The effective ion-ion pair potentials $U_{ij}$, equivalently called also ion-ion potentials of mean force (PMF) at infinite dilution which are input to our HNC calculations are derived from explicit-water MD simulations as described previously [19].

Briefly, we used the MD package GROMACS [38, 39] at constant particle number, pressure $P = 1$ bar, and a temperature $T = 300$ K using a Berendsen barostat and thermostat [40], respectively. The periodically repeated cubic simulation box included explicit ions and SPC/E water [41] and we applied the three dimensional particle-mesh Ewald (PME) summation method for the electrostatics. [42] Typical runs for gathering statistics were 150-200 ns in time after a $\simeq 5$ ns period of equilibration. The ions were modeled as charged and nonpolarizable Lennard-Jones (LJ) spheres. The LJ parameters, the energy $\epsilon$ and size $\sigma$ are those taken from Dang. [43–45] The cross interactions are calculated by the Lorentz-Berthelot mixing rules. For convenience, the resulting ion-water LJ parameters and the SPC/E parameters are summarized in Tab. II.

In order to derive accurate pair potentials between two ions (per definition at infinite

dilution) from the MD simulations it was made use of the fact that the short-ranged part of the ion-ion pair potential is concentration-independent up to c $\simeq$ 0.5 M [19, 46]. In the first step, accurate pair correlation functions $g(r)$ were calculated at a low, but non-vanishing concentration with sufficient statistics. After a finite-size correction of the $g(r)$s the PMF at the given concentration were obtained by a simple Boltzmann inversion ($\propto \ln[g(r)]$). The short-ranged part of the pair potential was derived by subtracting the non-specific Debye-Hückel contribution. For the total *infinite dilution* pair potential $U(r)$ the pure Coulomb interaction $\propto \lambda_B/r$ had to be added again. It was demonstrated that this procedure yields the identical short-ranged part of the pair potential for every density within a range from $c$ =0.025-0.5 M. Eventually, the infinite-dilution pair potentials in work [19] which are also used in this work to calculate thermodynamic properties were derived from a *single* simulation per salt type at a concentration of $c \simeq 0.3$ M. More details to the derivation of the PMFs, their particular forms, and related information can be found in previous work [19].

A necessary modification of the original PMFs is related to the inclusion of many-body effects: the virial route (Eq. 12) in MD is *not* exact as it employs the infinite dilution pair potential, and many-body contributions to the ion-ion interactions induced by water for higher densities are, therefore, not considered. As has been shown by Hess *et al.*, those contributions can be qualitatively corrected by taking into account the density-dependence of the water dielectric constant $\epsilon(c)$ [18]. The long-ranged $1/r$-Coulomb part in the pair potential $U_{ij}(r)$ between two ions having charges $z_i$ and $z_j$ has to be altered by using $\epsilon(c)$ instead of the limit $\epsilon(0)$, to obtain a corrected pair potential [17, 18]

$$\tilde{U}_{ij}(r;c) = U_{ij}(r) - \frac{z_i z_j}{r}\left[\lambda_B(0) - \lambda_B(c)\right], \tag{27}$$

where

$$\lambda_B(c) = \frac{\beta e^2}{4\pi\epsilon_0\epsilon(c)} \tag{28}$$

is the Bjerrum length in the aqueous electrolyte solution with concentration $c$.

It has been shown by Kalcher and Dzubiella that this correction leads to quantitative agreement of the virial route with the exact compressibility route for selected salts up to the concentration of 2 M within the statistical error. The necessary input parameter $\epsilon(c)$ is directly calculated from the all-atom MD simulations [19] and fitted by the function $\epsilon(c) = \epsilon(0)/(1 + Ac)$ with the values of the constant $A$ for different salts given in Table III.

For mixtures we assume the additive relation

$$\epsilon(c) = \epsilon(0)/(1 + \sum_{\alpha} A_{\alpha} c_{\alpha}), \tag{29}$$

summing over all salts present in the solution.

The implicit solvent treatment in HNC and MC methods does not consider the solvent-induced many body effects. To maintain internal consistency, we are using the concentration dependent pair potential $\tilde{U}_{ij}$ not only for the virial route osmotic coefficient (shown to work in implicit solvent calculations by Hess *et al.* [18]), but also for the compressibility route osmotic coefficient and activity coefficient.

**Thermodynamics from MD simulations**

Osmotic coefficients are obtainable from MD using PMFs and electrolyte structure by the two routes introduced before, namely the virial and compressibility route [19]. Briefly, the virial route (Eq. 12) involves both the PMFs and $g_{ij}(r)$s , directly calculated from the simulation. In contrast to HNC and MC using the solvent-averaged potentials, the $g(r)$s are in principle exact in MD. The many-body contributions to the PMF at higher density are not included. This is corrected with the concentration-dependent dielectric constant following the Eq. 27 and Table III.

In the compressibility route, we use an exact sum rule which relates the isothermal compressibility to a superposition of integrals over the $g(r)$s, the so-called Kirkwood-Buff factors [19, 31]. Eq. 18 is a reformulation of this sum rule in terms of the direct correlation function $c(r)$ and can be transformed to the form involving $g(r)$s using the Ornstein-Zernike equation (Eq. 3). The compressibility route in MD is thermodynamically exact but computationally cumbersome because of the integration of Eq. 17 as a function of electrolyte concentration [19]. For concentrations $c \lesssim 1$ M both routes showed quantitative agreement with each other while experimental results could be reproduced for the Cl salts only [19] showing deficiencies of the underlying MD force-fields used in this study.

**Thermodynamics from MC simulations**

Implicit solvent Metropolis Monte Carlo simulations are performed in the $NVT$ ensemble [47] using a cubic, periodic box using the minimum image convention. Salt particles

are randomly translated and the corresponding trial energy, $\Delta U$, determines if the move is accepted or not: if $\Delta U < 0$ the move is accepted and if $\Delta U > 0$ the move is accepted with the probability $\exp(-\beta\Delta U)$. The system energy is evaluated as the sum of all pair interactions, described using effective PMFs (resolution 0.1 Å), defined above (Eq. 27):

$$U = -\frac{1}{2}\sum_{i}^{N}\sum_{j}^{N}\tilde{U}_{ij}(r;c). \tag{30}$$

After equilibration, excess chemical potentials are sampled using the Widom particle insertion technique [48]. The energy of inserting a non-perturbing salt pair is sampled to obtain the ensemble average

$$\mu_{ex} = -\ln\left\langle \exp\left(-\beta\Delta U_{\text{pair}}\right)\right\rangle_0, \tag{31}$$

which is directly related to the *mean* activity coefficient, $\gamma_{\pm} = \exp\left(\mu_{ex}/2\right)$. Depending on the salt concentration, the number of particles in the simulation box varies between 20–1000, with $10^6$ configurations per particle generated during the production runs. Octupling the number of particles does not change the results significantly. We sample the above average every tenth configuration.

Within the primitive model of electrolytes the described method has proven accurate for determining activity coefficients in a large range of salt solutions [37] as well as in multicomponent mixtures including sea water [16].

The osmotic coefficient, $\Phi$, is obtained via the virial equation for the pressure [49, 50] (see also Eq. 12)

$$\Phi = 1 + \frac{\left\langle \sum_{i\neq j}\mathbf{f}(\mathbf{r_{ij}})\cdot\mathbf{r_{ij}}\right\rangle_{N,V,T}}{3NkT}, \tag{32}$$

where $\mathbf{f}(\mathbf{r_{ij}})$ is the force between particle $i$ and $j$, calculated by numerical differentiation of the pair potential.

The source code of the MC simulation program is available via the Faunus project [51].

## RESULTS

In the following we summarize the results obtained using our hybrid HNC/MD approach and infinite dilution PMFs, in comparison with results of implicit solvent MC calculations (denoted only MC in the following) employing the same pair potentials, with results of recently published MD simulations [19], and with experimental data, where available. We

are interested in structural properties (radial distribution functions), osmotic coefficients and excess chemical potentials (activity coefficients), which will now be discussed separately. All HNC and MC calculations were performed at the temperature of 300 K, employing the concentration-dependent dielectric constant in the pair potential, as described in the methodological section.

**Simple electrolytes**

Using the Ornstein-Zernike equation with the HNC closure relation, we calculated properties of a series of simple aqueous electrolyte solutions (with water treated in a solvent-averaged way), namely LiCl, NaCl, KCl, CsCl, NaI, and KF.

*Electrolyte structure*

Figure 1 shows a comparison of cation-anion pair correlation functions $g(r)_{\pm}$ for all studied salts at three different concentrations – 0.3, 1 and 2 M – as obtained from MD and MC simulations and the HNC calculation. The HNC and MC curves show excellent agreement in all cases. There are, though, some differences to the explicit solvent MD curves. This tells us that the approximative treatment of the statistical mechanics in the HNC theory is not the main approximation made here (since it provides the same results with the PMFs as the inherently non-approximative MC calculation). The differences apparently arise from the reduction of the many-body interactions thta are present in MD to the effective pair potentials in HNC and MC.

The weakly hydrated ion pairs CsCl and KCl show the best agreement among all three theoretical methods used. A small disagreement between MD and primitive model calculations is observed for KF, LiCl, NaCl, and NaI, where at least one ion is relatively small and thus strongly hydrated ($Li^+$, $Na^+$, and $F^-$). This finding suggests that for the latter ions the explicit inclusion of hydration effects indeed is more important for describing the structure at nonvanishing concentrations. We find that the same conclusions can be drawn from the structure between anion-anion and cation-cation pairs, even though the quantitative agreement between HNC/MC and MD is better in these cases (plots not shown).

The good overall agreement between HNC, MC (both implicit solvent) and MD (explicit

solvent) demonstrates that the approximative HNC closure using infinite dilution PMFs from MD simulations is capable of providing reliable structural information. It can therefore be expected that it will also perform well for the evaluation of thermodynamic properties, which is the subject of the following section.

*Osmotic coefficients*

The experimental values [52, 53] of the osmotic coefficient $\Phi$ for the studied salts as well as results of our HNC, MD [19], and MC calculations are shown in Fig. 2. The results of the HNC and MC calculations were converted from the MM to the LR level using Eq. 25 (see the Methodology section for details). Regarding $\Phi$, the chloride series shows a classical Hofmeister ordering which in this case displays a monotonic decrease of $\Phi$ with increasing cation size. As was noted before, we obtain the osmotic coefficients from the HNC calculation by two routes, the virial and compressibility route. The outcomes of these two approaches will be discussed separately.

The error bars in our HNC calculations originating from the uncertainty in the PMFs were found to be lower than $\pm 5\,\%$ at 1 mol/kg (see supplementary information). The absolute error $\Phi$ of the implicit model (relative to MD) is roughly of the order of 0.1 (concentration range 0.5-1.5 mol/kg) due to the small differences between MD and HNC/MC $g(r)$s and the large sensitivity of the osmotic coefficient to the structural data and the exact form of the pair potential [8, 17, 19, 54, 55]. The increasing quantitative deviation between MD and implicit methods for larger concentrations (above 1 mol/kg) is also to be expected due to the solvent-averaged treatment of the latter. As was shown in the section devoted to the electrolyte structure, the effect of the HNC approximation itself is in our case much smaller than the neglect of the explicit solvent.

*Virial route*: The calculated osmotic coefficients from HNC, MD, and MC calculations using the virial route (Eq. 12) are shown in Figs. 2a, 2b, and 2c, respectively. As can be seen, the curves are very similar. Both implicit solvent calculations, HNC and MC, show perfect agreement. Explicit MD simulations (Fig. 2b) show different ordering of the curves for LiCl/NaCl and KCl/CsCl. The differences, however, lie within the statistical error of the calculations. Deviations between MC and HNC on one hand and MD on the other hand for NaI are more pronounced.

As was noted by Kalcher *et al.* [19], the comparison of MD osmotic coefficients (Fig. 2b) with the experimental values (Fig. 2f) and trends was favorable for LiCl, NaCl, and CsCl for moderate densities - the values lie within the error bars of the MD calculation. The same applies to HNC and MC osmotic coefficients (Figs. 2a,c). The results for KF show incorrect behavior for all three approaches which indicates a problem in the MD force-field used for the infinite dilution PMF calculation [19]. NaI coefficients are slightly too large in HNC and MC (Figs. 2a, c) and much larger in MD (Fig. 2b) – here the solvent averaged treatment (accidentally) provides better agreement with experiment than MD calculations.

Fig. 3 compares the virial route (Eq. 12) osmotic coefficients for all three methods (MD, HNC, MC) and experimental data for a fixed molality of 1 mol/kg. The coefficients from MC and HNC agree almost perfectly with each other. The MD values are slightly different, with the largest deviation observed for NaI. As argued before, deviations to experiments for these salts very likely stem from a faulty force-field used in the MD.

*Compressibility route:* The calculated osmotic coefficients from the HNC and MD calculations using the compressibility route (Eqns. 17 and 18) are shown in Figs. 2d and 2e. The previous discussion can be fully extended to the compressibility route as well, since the results are qualitatively, and to a large extent quantitatively the same. The differences in MD and HNC ordering observed for LiCl and NaCl lie within the error bars of the calculation.

*Comparison of approaches towards* $\Phi$*:* As can be seen from the comparison of the data in Figs. 2 and 3, the osmotic coefficients calculated using the HNC method (Figs. 2a, d) qualitatively do not depend on the thermodynamic route used. There is a quantitative difference for all salts, namely all curves coming from the HNC compressibility route are slightly ($\sim$ 10%) higher than their virial counterparts. This difference comes probably from the known fact that the approximative integral equation closures are in general not thermodynamically consistent [26].

Fig. 4 compares the experimental and calculated osmotic coefficients of LiCl and CsCl in the whole studied concentration range, making also the assessment of the spread in the calculated curves easier. The theoretical curves lie within the errorbars of the respective calculations, are consistent with each other, and provide excellent agreement among the different theoretical approaches used.

We conclude this section by stating that the description of the osmotic coefficient is, within the errorbars of the calculation, consistent among all the approaches used in this study

(HNC, MC, MD and virial/compressibility routes). The disagreement with the experimental data is to be associated with the incorrect parametrization of the underlying MD force-field for KF and of NaI (even though the HNC/MC osmotic coefficients for this salt compare relatively well with the experiment).

*Activity coefficients*

The comparison of HNC and MC results (converted from MM to LR level using Eq. 26) for the activity coefficient without the Born correction (Eq. 24) with experiments [33] is given in Fig. 5. The error bars in our HNC calculations originating from the uncertainty in the PMFs were found to be slightly larger that those of the osmotic coefficients – in the order of $\pm 5\,\%$ at 1 mol/kg (see supplementary information).

HNC and MC data calculated using Eqns. 20 and 31, respectively (Figs. 5a-b) compare very well to each other, particularly in the lower concentration range. The largest deviations are observed for LiCl at concentrations above 1 mol/kg. Quantitative agreement with experimental data (Fig. 5c) is poor, the spread in the calculated data is too large. At this step, NaCl and NaI are described consistently in the solvent averaged theory and in experiments. LiCl and KF are qualitatively wrong.

As was discussed above, we need to correct the mean activity coefficients because of the concentration-dependent dielectric constant $\epsilon(c)$. The machinery used for this purpose was described in the Methodology. It involves multiplying the calculated mean activity coefficient $\gamma_\pm$ (Eq. 22) with the Born solvation energy contribution (Eqns. 23 and 24). The corrected HNC curves are shown in Figs. 5d-e for two different sizes of the ion radii used for the Born energy evaluation (effective and solvated radii, respectively, shown in Table I).

The first thing to note is that the Born correction is quite substantial. In some cases and at larger concentration it more than doubles the non-corrected activity coefficient, particularly with the effective ionic radii $a^{\text{eff}}$ used in the calculation. As a result, the salts whose (uncorrected) coefficients were too low but qualitatively more or less consistent with experiment (KCl, CsCl) are described better using the corrected values. The coefficients of NaCl and NaI, on the other hand, are way too high. Thanks to the cancellation of different effects, the corrected $\gamma_\pm$ of LiCl quantitatively agrees with the experimental data when the solvated ion radii are used in the Born energy calculation.

Fig. 6 compares the experimental and calculated mean activity coefficients of LiCl and CsCl in the whole studied concentration range. The results confirm the importance of the Born corrections and indicate that using the solvated ionic radii for its evaluation is a step in the right direction. However, this selection of the radii is not unambiguous and has to be treated as a fitting parameter at the moment. Using the radius of the solvated ions plus the first solvation shell should give a more accurate representation of the Born energy, since the water molecules in the first solvation shell are saturated and the dielectric response will not react to the salt concentration in the solution. It is, therefore, not surprising that the larger radii give a somewhat better representation of the experimental activity coefficients. Clearly, more work along these lines is needed.

**Multicomponent electrolyte mixtures**

The OZ equation (Eq. 3) allows for easy extension of the number of components in the studied mixture just by introducing the respective correlation functions and particle densities. We extended our calculations to mixtures of salts, while employing the same PMFs as for the 1:1 electrolytes. In addition, MD calculations of mixed cation-cation PMFs have been performed for this part of our study.

The results for 2 mixtures – LiCl/NaCl and NaCl/KCl – are displayed in Fig. 7, where we plot $\Phi$ for a fixed total solution concentration (ionic strength) versus the molar fraction $x$ of one of the salts. In this case, the osmotic coefficients were not converted to the LR level (Eq. 25) because of the unavailability of reliable density data. The dielectric constants of the mixtures were estimated using the dielectric constants of the pure salt solutions (Eq. 29).

The values of the osmotic coefficients of a given mixture at a constant total concentration lie between the osmotic coefficients of the solutions constituent salts at the same concentration. The trends observed in Fig. 7 for different total solution concentrations are consistent with the results of the calculations of individual salts.

For LiCl/NaCl mixtures, a small curvature (non-linearity) can be observed in the constant total concentration plots, which is discernible due to the fact that the calculated $\Phi$ of pure LiCl and NaCl solutions lie very close to each other. For NaCl/KCl, where the calculated osmotic coefficient of the individual salts are quite different, the constant total concentration plot shows linear behavior.

The comparison with experimental data is complicated for several reasons: a) the agreement of the calculated osmotic coefficients of individual salts with experiment is not precise enough in order to draw decisive conclusions; b) the experimental data (given almost exclusively at constant molar ratio) are usually sparse and at too high concentrations.

Anyway, the trends in the ordering of the calculated values seem to be consistent with the experiments [56–60]. We plan to carry out more detailed study of electrolyte mixtures as soon as we have the PMFs available, which describe the behavior of simple solutions accurately.

## SUMMARY

We presented here the results of our combined HNC/MD study employing PMFs of individual ions at infinite dilution as pair potentials. This method provides results consistent with the full atom and explicit solvent MD treatment. The versatility of our method was demonstrated by its application to the study of mixtures of two binary electrolytes. Further extension to more complicated multicomponent systems is also possible.

The validity of the HNC calculations was confirmed by implicit solvent MC simulations involving the same (solvent-averaged) pair potentials. Both methods provide the same structural (pair correlation functions $g(r)$) and thermodynamic information (osmotic coefficients $\Phi$, mean activity coefficients $\gamma_{\pm}$) indicating that the approximations within the HNC method do not play any significant role for the systems and concentration range we studied. When we compared the $g(r)$s based on solvent-averaged potentials with the MD data obtained with explicit solvent, we observed minor differences for salts involving strongly hydrated ions ($Li^+$, $Na^+$, $F^-$) – the effective treatment of the solvent molecules and the neglect of the (solvent-induced) many-body interactions in the pair potentials is clearly the approximation affecting the results the most.

The osmotic coefficients $\Phi$ are described consistently among the different methods (explicit solvent MD; implicit solvent HNC and MC) and thermodynamic approaches (virial vs. compressibility route). The values provided by the HNC and MC are in almost perfect agreement. The differences to the MD treatment lie mostly within the statistical error of the calculations. As reported earlier [19], the comparison with the experimental data is favorable for LiCl, NaCl and CsCl. It is apparent that the disagreement with the experiments for the

other salts is caused by the faulty MD force-field used for the PMF calculation and not by the approximations used in the implicit-solvent methods.

We have shown that the mean activity coefficients are described consistently within the solvent-averaged HNC and MC calculations. The agreement of the Born-uncorrected HNC and MC mean activity coefficients with experimental data is rather poor and does not correlate with the outcome of the osmotic coefficient calculations. As was shown for the case of HNC $\gamma_{\pm}$, due to the use of the concentration dependent dielectric constant $\epsilon(c)$, it is necessary to introduce the correction of the excess chemical potential (and, therefore, also of the mean activity coefficient) by means of the Born energy contribution. This contribution, which has to be taken into account for all implicit solvent based models and which was found to play a rather decisive role in the evaluation of the activity coefficient, unfortunately includes one parameter (the ionic radius) whose evaluation is not unambiguous.

It is apparent from the results that the modeling of activity coefficients is much more complicated than that of osmotic coefficients. We thus conclude that the osmotic coefficients are less error-prone and more suitable for the studies using implicit-solvent models.

We want to emphasize once more that the solvent-averaged infinite dilution potential (PMF) provides enough information, in order to allow good description of structural and thermodynamic properties of salt solutions in the moderate concentration range (0-2 M). The critical condition here is the quality and accuracy of the pair potential (PMF), which can have large effects on the resulting thermodynamic properties. This bottleneck can, nonetheless, be overcome by the growing availability of computational resources.

Our method has very high benefit/cost ratio by providing data qualitatively and quantitatively consistent with explicit solvent simulations, but being much faster (HNC calculation is finished within minutes). It can be also easily used for multicomponent mixtures. The evaluation of thermodynamic properties is much more straightforward in the HNC, when compared to MD.

This approach allows also for a very efficient MD force-field optimization and development. Ionic force-field development is typically based on single ion properties such as the solvation free energy [61]. In our method a quick assessment of the thermodynamic validity of the proposed force-field for a wide range of electrolyte concentrations is possible. In other words, after an ionic interaction parameter set is designed and infinite-dilution PMFs are generated from MD, they are used in the HNC machinery. The thermodynamic results can

be compared to experiments and the input parameters can be adjusted and tested in the next round in order to obtain better consistency with existing reference data.

LV is grateful to the Alexander von Humboldt Foundation for the financial support. JD and IK thank the Deutsche Forschungsgemeinschaft (DFG) for support within the Emmy-Noether-Program, and the Leibniz-Rechenzentrum (LRZ) München for computing time on HLRB II. We acknowledge the German Arbeitsgemeinschaft industrieller Forschungvereinigungen Otto von Guericke e.V. (AiF) in the framework of the project 'Simulation and prediction of salt influence on biological systems'. ML thanks the Linneaus Center of excellence "Organizing Molecular Matter" for financial support.

* Electronic address: lubos@vrbka.net

† Electronic address: mikael.lund@teokem.lu.se

‡ Electronic address: jdzubiel@ph.tum.de

[1] P. Debye and E. Hückel, Physikalische Zeitschrift **24**, 185 (1923).

[2] K. S. Pitzer, Journal of the American Chemical Society **102**, 2902 (1980).

[3] E. Waisman and J. C. Lebowitz, Journal of Chemical Physics **56**, 3086 (1972).

[4] L. Blum, Molecular Physics **30**, 1529 (1975).

[5] J.-P. Simonin, L. Blum, and P. Turq, Journal of Physical Chemistry **100**, 7704 (1996).

[6] N. Papaiconomou, J.-P. Simonin, O. Bernard, and W. Kunz, Physical Chemistry and Chemical Physics **4**, 4435 (2002).

[7] N. Papaiconomou, J.-P. Simonin, O. Bernard, and W. Kunz, Journal of Molecular Liquids **113**, 5 (2004).

[8] P. S. Ramanathan and H. L. Friedman, Journal of Chemical Physics **54**, 1086 (1971).

[9] P. G. Kusalik and G. N. Patey, Journal of Chemical Physics **92**, 1345 (1990).

[10] C. P. Ursenbach, D. Wei, and G. N. Patey, Journal of Chemical Physics **94**, 6782 (1991).

[11] J.-P. Simonin, O. Bernard, N. Papaiconomou, and W. Kunz, Fluid Phase Equilibria **264**, 211 (2008).

[12] C. Held, L. F. Cameretti, and G. Sadowski, Fluid Phase Equilibria **270**, 87 (2008).

[13] C. Held and G. Sadowski, Fluid Phase Equilibria **279**, 141 (2009).

[14] G. I. Szasz, W. Dietz, K. Heinzinger, G. Pálinkás, and T. Radnai, Chemical Physics Letters

**92**, 388 (1982).

[15] E. Spohr, G. Pálinkás, K. Heinzinger, P. Bopp, and M. M. Probst, Journal of Physical Chemistry **92**, 6754 (1988).

[16] M. Lund, B. Jönsson, and T. Pedersen, Marine Chemistry **80**, 95 (2003).

[17] B. Hess, C. Holm, and N. van der Vegt, Journal of Chemical Physics **124**, 164509 (2006).

[18] B. Hess, C. Holm, and N. van der Vegt, Physical Review Letters **96**, 127801 (2006).

[19] I. Kalcher and J. Dzubiella, Journal of Chemical Physics **130**, 134507 (2009).

[20] W. Kunz, P. Turq, M.-C. Bellissent-Funel, and P. Calmettes, Journal of Chemical Physics **95**, 6902 (1991).

[21] H. Krienke, V. Vlachy, G. Ahn-Ercan, and I. Bakó, Journal of Physical Chemistry B **113**, 4360 (2009).

[22] A. P. Lyubartsev and S. Marčelja, Physical Review E **65**, 041202 (2002).

[23] *Scientific tools for Python* (2009), URL `http://www.scipy.org`.

[24] L. Vrbka, *OZ-solver in Python* (2009), URL `http://www.pyoz.vrbka.net`.

[25] W. G. McMillan and J. E. Mayer, Journal of Chemical Physics **13**, 276 (1945).

[26] J.-P. Hansen and I. R. McDonald, *Theory of simple liquids* (Academic Press, 2005).

[27] L. S. Ornstein and F. Zernike, Proceedings of the Academy of Science (Amsterdam) **17**, 793 (1914).

[28] K.-C. Ng, Journal of Chemical Physics **61**, 2680 (1974).

[29] J. C. Rasaiah and H. L. Friedman, Journal of Chemical Physics **48**, 2742 (1968).

[30] J. P. Hansen, G. M. Torrie, and P. Vieillefosse, Physical Reviews A **16**, 2153 (1977).

[31] R. Kjellander and S. Sarman, Journal of Chemical Physics **90**, 2768 (1989).

[32] L. Verlet and D. Levesque, Physica **28**, 1124 (1962).

[33] R. A. Robinson and R. H. Stokes, *Electrolyte Solutions* (Butterworths Scientific Publications, London, 1959).

[34] H. L. Friedman, Journal of Solution Chemistry **1**, 387 (1972).

[35] J. P. Simonin, Journal of the Chemical Society, Faraday Transactions **92**, 3519 (1996).

[36] C. A. Haynes and N. J., Fluid Phase Equilibria **145**, 255 (1998).

[37] Z. Abbas, E. Ahlberg, and S. Nordholm, Fluid Phase Equilibria **260**, 233 (2007).

[38] H. J. C. dsen, D. van der Spoel, and R. van Drunen, Computer Physics Communications **91**, 43 (1995).

[39] E. Lindahl, B. Hess, and D. van der Spoel, Journal of Molecular Modeling **7**, 306 (2001).

[40] H. J. C. Berendsen, J. P. M. Postma, W. F. van Gunsteren, A. DiNola, and J. R. Haak, Journal of Chemical Physics **81**, 3684 (1984).

[41] H. J. C. Berendsen, J. R. Grigera, and T. P. Straatsma, Journal of Physical Chemistry **91**, 6269 (1987).

[42] U. Essmann, L. Perera, M. L. Berkowitz, T. Darden, H. Lee, and L. G. Pedersen, Journal of Chemical Physics **103**, 8577 (1995).

[43] L. X. Dang, Journal of Chemical Physics **96**, 6970 (1992).

[44] L. X. Dang and B. C. J. Garrett, Journal of Chemical Physics **99**, 2972 (1993).

[45] L. X. Dang, Journal of American Chemical Society **117**, 6954 (1995).

[46] J. Perkyns and B. M. Pettitt, Journal of Chemical Physics **97**, 7656 (1992).

[47] N. A. Metropolis, A. W. Rosenbluth, M. N. Rosenbluth, A. Teller, and E. Teller, Journal of Chemical Physics **21**, 1087 (1953).

[48] B. Widom, Journal of Chemical Physics **39**, 2808 (1963).

[49] D. Frenkel and B. Smit, *Understanding Molecular Simulation* (Academic Press, 2001), 2nd ed., ISBN 0122673514.

[50] D. A. McQuarrie, *Statistical Mechanics* (University Science Books, 2000), 2nd ed.

[51] M. Lund, M. Trulsson, and B. Persson, Source Code for Biology and Medicine **3**, 1 (2008).

[52] A. Heydweiller, Annalen der Physik **335**, 873 (1910).

[53] W. J. Hamer and Y.-C. Wu, Journal of Physical and Chemical Reference Data **1**, 1047 (1972).

[54] B. M. Pettitt and P. J. Rossky, Journal of Chemical Physics **84**, 5836 (1986).

[55] T. Åkesson, C. Woodward, and B. Jönsson, J. Chem. Phys. **91**, 2461 (1989).

[56] R. A. Robinson and C. K. Lim, Transactions of the Faraday Society **49**, 1144 (1953).

[57] M. A. Flesia, M. R. G. de Chialvo, and A. C. Chialvo, Fluid Phase Equilibria **131**, 189 (1997).

[58] H. F. Holmes, J. C. F. Baes, and R. E. Mesmer, Journal of Chemical Thermodynamics **11**, 1035 (1979).

[59] H. F. Holmes and R. E. Mesmer, Journal of Chemical Thermodynamics **20**, 1049 (1988).

[60] A. Dinane, M. E. Guendouzi, and A. Mounir, Journal of Chemical Thermodynamics **34**, 423 (2002).

[61] D. Horinek, S. I. Mamatkulov, and R. R. Netz, Journal of Chemical Physics **130**, 124507 (2009).

| ion | radius (Å) | |
|---|---|---|
| | $a^{\mathrm{eff}}$ | $a^{\mathrm{solv}}$ |
| $Li^+$ | 1.96 | 4.25 |
| $Na^+$ | 2.45 | 4.55 |
| $K^+$ | 2.82 | 4.90 |
| $Cs^+$ | 3.11 | 5.10 |
| $F^-$ | 2.64 | 4.50 |
| $Cl^-$ | 3.22 | 4.95 |
| $I^-$ | 3.61 | 5.25 |

TABLE I: Ionic radii used for the estimation of the Born contribution to the excess chemical potential. Effective radii of solvated ions ($a^{\mathrm{eff}}$, position of the first maximum in the $g(r)$) and radii of solvated ions including the first solvation shell ($a^{\mathrm{solv}}$, position of the second maximum in the $g(r)$) are given [19].

| Ion | $\sigma_{iO}$(nm) | $\epsilon_{iO}$(kJ/mol) | charge $q/e$ |
|---|---|---|---|
| $Li^+$ | 0.2337 | 0.6700 | +1 |
| $Na^+$ | 0.2876 | 0.5216 | +1 |
| $K^+$ | 0.3250 | 0.5216 | +1 |
| $Cs^+$ | 0.3526 | 0.5216 | +1 |
| $Cl^-$ | 0.3785 | 0.5216 | -1 |
| $F^-$ | 0.3143 | 0.6999 | -1 |
| $I^-$ | 0.4168 | 0.5216 | -1 |
| SPC/E | | | |
| O | 0.3169 | 0.6500 | -0.8476 |
| H | – | – | +0.4238 |

TABLE II: Ion-water oxygen (O) LJ parameters and charges used in our work.

| salt | $A^{MD}$ ($mol^{-1}$) | $A^{exp}$ ($mol^{-1}$) |
|---|---|---|
| LiCl | 0.31 | 0.232 |
| NaCl | 0.27 | 0.223 |
| KCl | 0.24 | 0.184 |
| CsCl | 0.23 | 0.152 |
| NaI | 0.34 | 0.229 |
| KF | 0.19 | 0.136 |

TABLE III: Values of the constant $A$ for the evaluation of the concentration-dependent dielectric constant using the expression $\epsilon(c) = \epsilon(0)/(1 + Ac)$ as obtained from MD simulations [19] and from experimental data.

FIG. 1: Comparison of cation-anion $g(r)$s for all studied salts in 0.3M, 1.0M and 2.0M solutions. (top row from left to right LiCl, NaCl, KCl; bottom row from left to right CsCl, NaI, KF). Note that the curves for 1M and 2M solutions were shifted to the right by 0.5 and 1 Å, respectively.

FIG. 2: Osmotic coefficients calculated (at the LR level) via the virial (top, Eq. 12) and the compressibility (bottom, Eq. 18) route, coming from HNC (left) and MD simulations [19] (center). Results of MC calculations with the virial route (c) and experimental data (f) are given as well.

FIG. 3: Experimental and calculated (virial route) osmotic coefficients at the concentration of 1 mol/kg for all studied salts.

FIG. 4: Comparison of experimental and calculated osmotic coefficients $\Phi$ for LiCl (left) and CsCl (right) in the whole concentration range. The labels *vir* and *cmp* denote the data obtained via virial and compressibility route, respectively.

FIG. 5: Mean activity coefficients of studied salts from HNC (a), MC (b) – both Born-uncorrected, and experiment (c). The Born-corrected HNC curves are given for bare ion radii (d) and solvated radii (e).

FIG. 6: Comparison of experimental and calculated mean activity coefficients $\gamma_{\pm}$ for LiCl (left) and CsCl (right) in the whole concentration range. The curves *HNC* and *MC* show Born-uncorrected data. The labels *Bb* and *Bs* denote the data including the Born correction with effective and solvated radii, respectively.

FIG. 7: Osmotic coefficients of LiCl/NaCl (left) and NaCl/KCl (right) electrolyte mixtures. Curves presented are calculated at constant total molar concentration and not converted from the MM to the LR level.

Figure 1

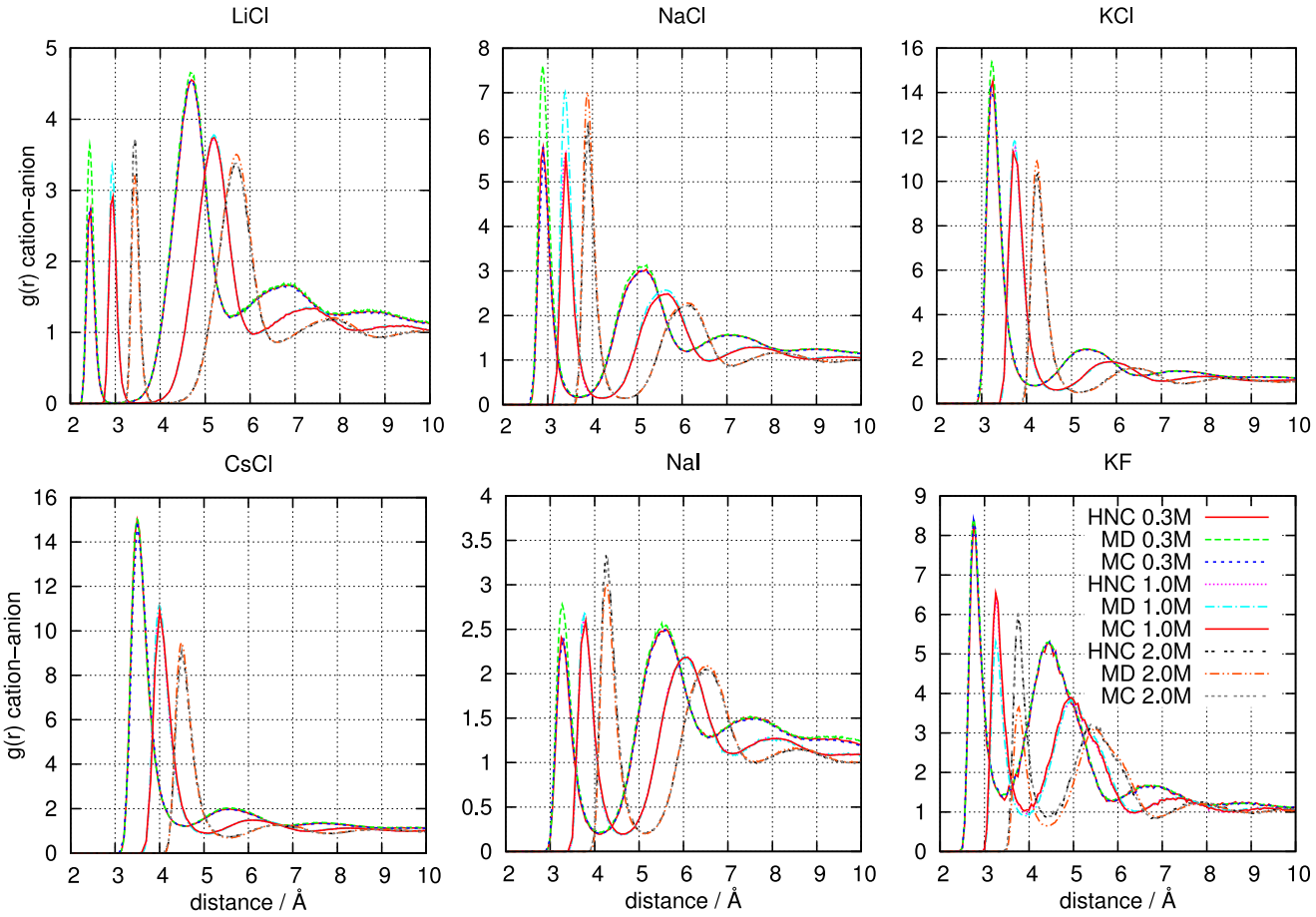
LiCl
NaCl
KCl
CsCl
NaI
KF
g(r) cation–anion
distance / Å
HNC 0.3M
MD 0.3M
MC 0.3M
HNC 1.0M
MD 1.0M
MC 1.0M
HNC 2.0M
MD 2.0M
MC 2.0M

Figure 2

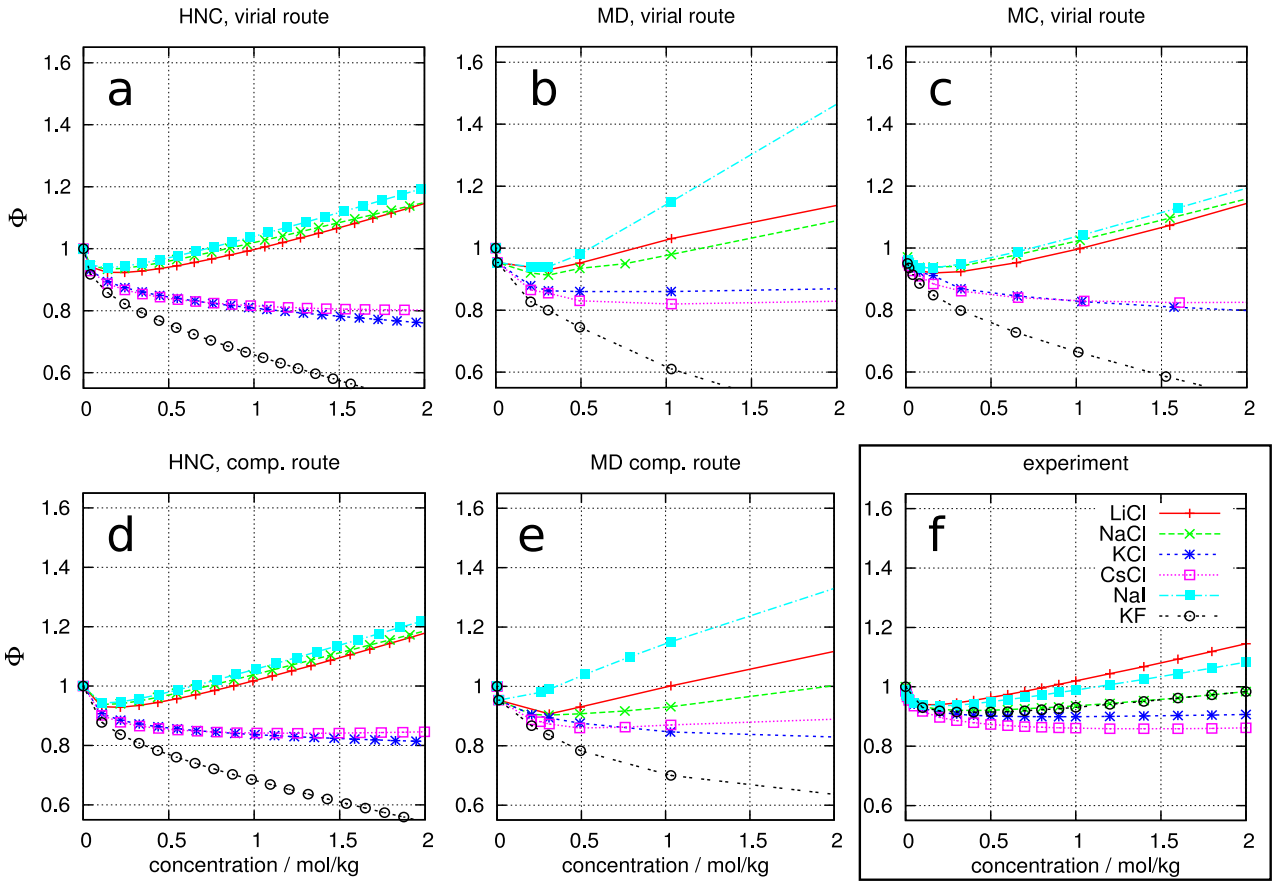
HNC, virial route
MD, virial route
MC, virial route
HNC, comp. route
MD comp. route
experiment
a
b
c
d
e
f
Φ
concentration / mol/kg
LiCl
NaCl
KCl
CsCl
NaI
KF

Figure 3

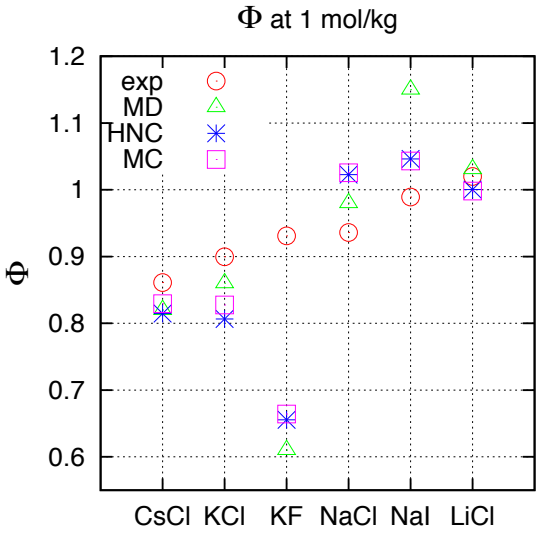
Φ at 1 mol/kg
exp
MD
HNC
MC
Φ
1.2
1.1
1
0.9
0.8
0.7
0.6
CsCl
KCl
KF
NaCl
NaI
LiCl

Figure 4

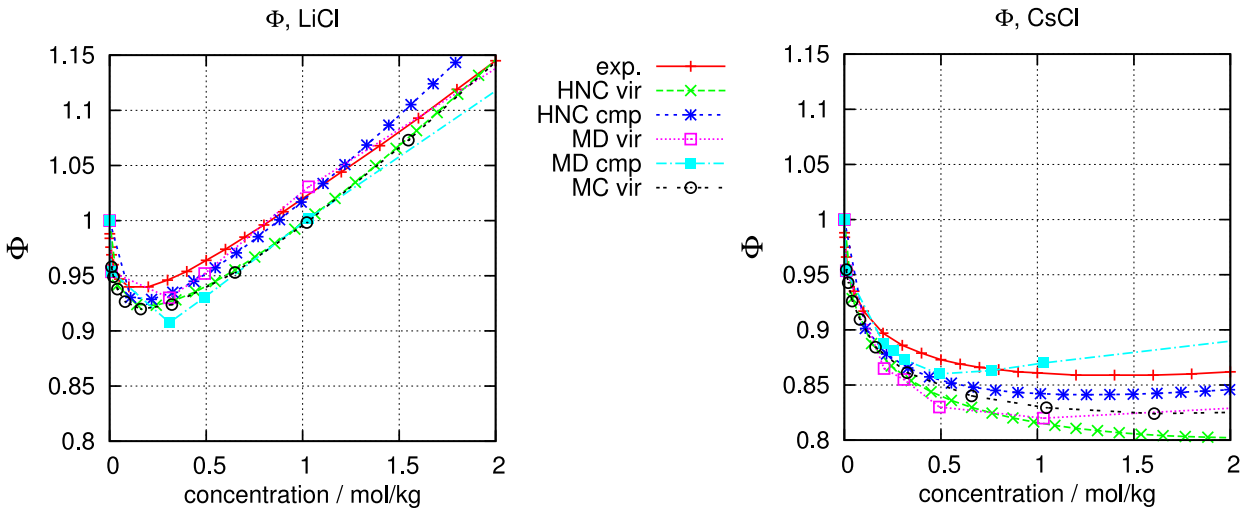
Φ, LiCl
Φ, CsCl
exp.
HNC vir
HNC cmp
MD vir
MD cmp
MC vir
Φ
concentration / mol/kg
1.15
1.1
1.05
1
0.95
0.9
0.85
0.8
0
0.5
1
1.5
2

Figure 5

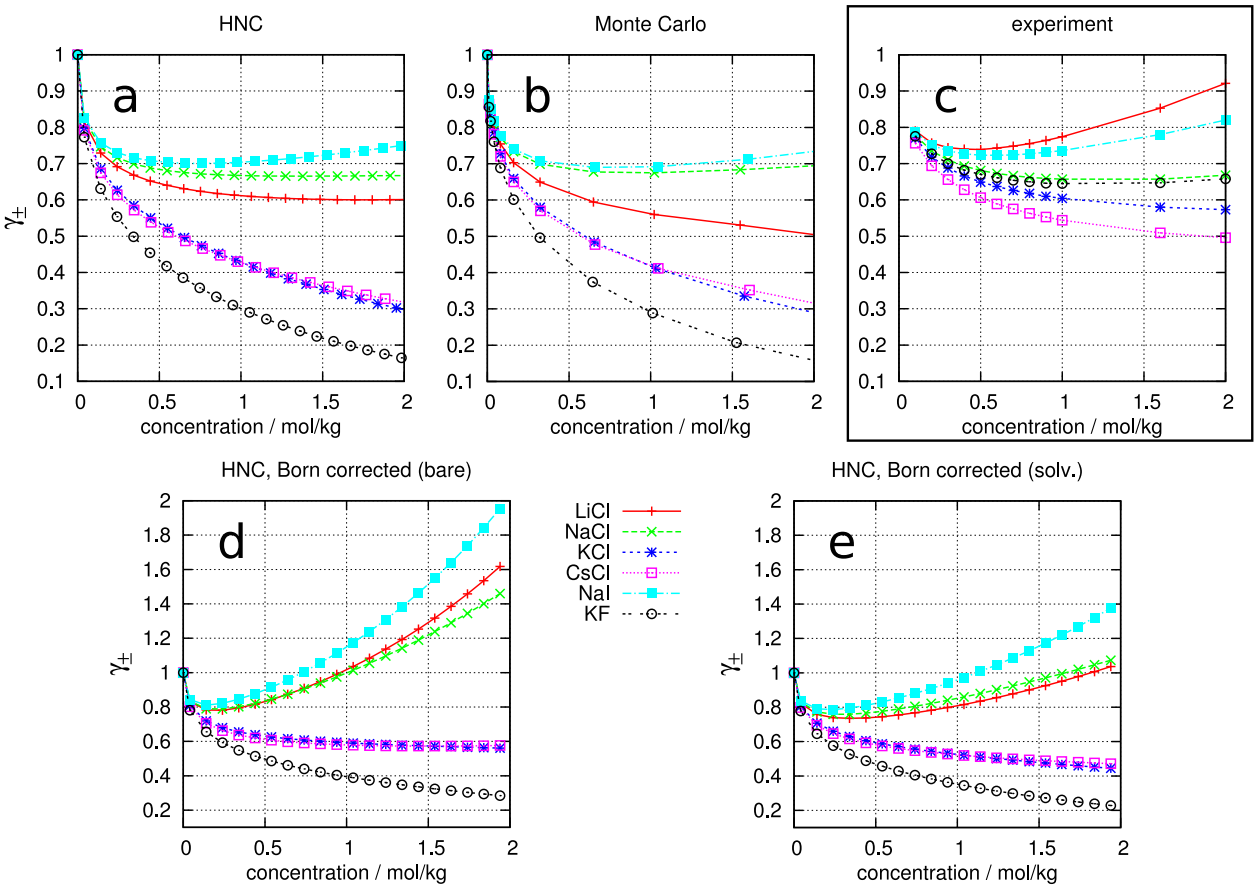
HNC
Monte Carlo
experiment
a
b
c
d
e
$\gamma_\pm$
concentration / mol/kg
HNC, Born corrected (bare)
HNC, Born corrected (solv.)
LiCl
NaCl
KCl
CsCl
NaI
KF

Figure 6

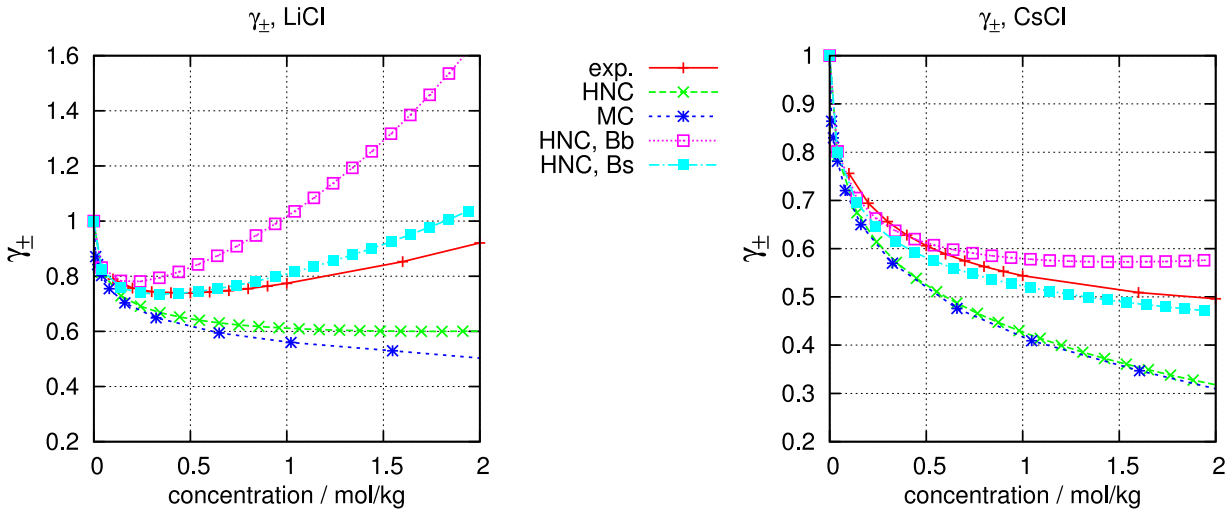
γ±, LiCl
1.6
1.4
1.2
1
0.8
0.6
0.4
0.2
γ±
0
0.5
1
1.5
2
concentration / mol/kg
exp.
HNC
MC
HNC, Bb
HNC, Bs
γ±, CsCl
1
0.9
0.8
0.7
0.6
0.5
0.4
0.3
0.2
γ±
0
0.5
1
1.5
2
concentration / mol/kg

Figure 7

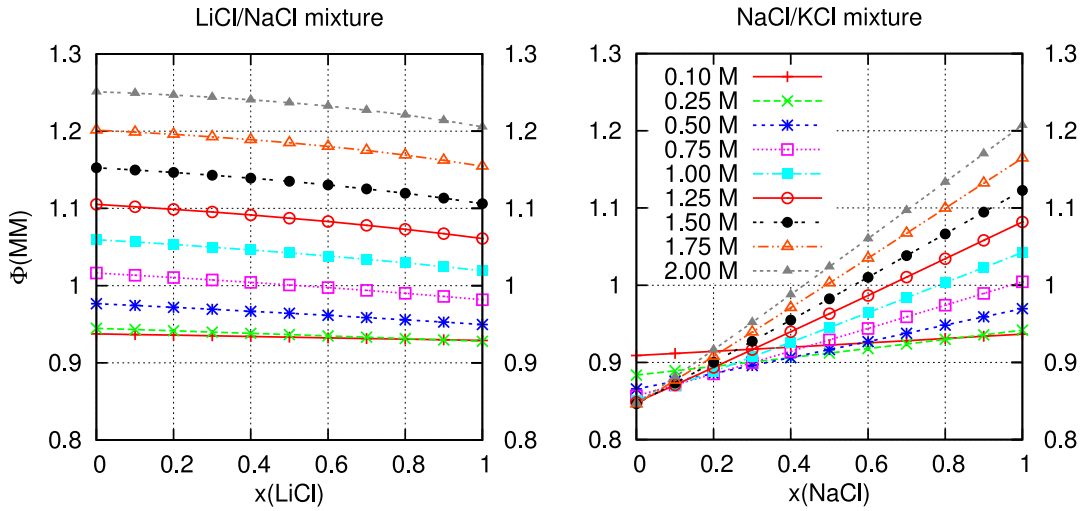
LiCl/NaCl mixture
NaCl/KCl mixture
Φ(MM)
x(LiCl)
x(NaCl)
0.10 M
0.25 M
0.50 M
0.75 M
1.00 M
1.25 M
1.50 M
1.75 M
2.00 M

## SUPPLEMENTARY INFORMATION

In order to evaluate the error associated with the uncertainity in the PMFs coming from the MD simulations [19], we performed for NaCl additional calculations with the pair potentials corresponding to the lower and upper bounds of the PMF uncertainity. The results of the evaluation of the osmotic and activity coefficients coming from these two extreme cases, together with the values corresponding to the mean PMFs are given in Fig. 8.

It turns out that the error in both cases increases with increasing concentration. Also, the error in $\Phi$ is slightly smaller than the error in $\gamma_{\pm}$. Anyway, in both cases, it is estimated to be close to $\pm 5\,\%$ at the concentration of 1 mol/kg.

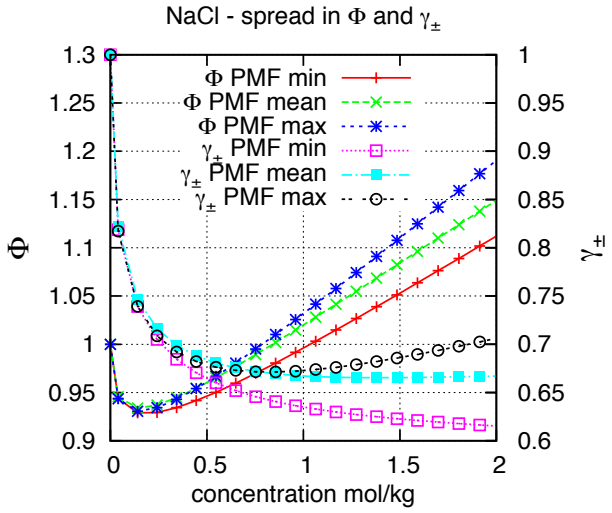


FIG. 8: Spread in osmotic and (Born-uncorrected) activity coefficients of NaCl, calculated using the HNC approximation with pair potentials corresponding to lower and upper bound of the PMF uncertainty and to the mean value of the PMF [19].